Solid Freeform Fabrication 2019: Proceedings of the 30th Annual International
Solid Freeform Fabrication Symposium – An Additive Manufacturing Conference
Reviewed Paper

Investigating the build consistency of a laser powder bed fused nickel-based superalloy, using the small punch technique

Authors: B. Haigh[1], R.J. Lancaster[1], R. Johnston[1], M. White[2] and J. Minshull[2]

[1] Institute of Structural Materials, Bay Campus, Swansea University, Swansea, SA1 8EN

[2] GKN Additive, Golf Course Lane, Filton, Bristol, BS34 9AU

Keywords

Inconel 718, laser powder bed fusion, small punch, microstructure, porosity

Abstract

Inconel 718 (IN718) is a nickel-based superalloy that possesses impressive corrosion resistance and high strength properties at elevated temperatures, making it an ideal choice for aerospace applications. However, with the continuous evolution of the jet engine, there is a strong desire to fabricate more intricate components with less stress-raising features to enable higher engine efficiencies to be achieved. To overcome this issue, aerospace engineers are looking at Additive Manufacturing (AM) as a potential solution. A limitation of AM is the transient nature of the microstructure, and it is difficult to produce representative laboratory scale mechanical test specimens that closely replicate the microstructure of the finished component. Therefore, it can be beneficial to utilise small-scale test methods, such as the Small Punch (SP) test, which can obtain mechanical property information from miniaturised specimens extracted directly from the finished part. In this paper, the small punch test technique has been adopted to characterise and evaluate the mechanical response of laser powder bed fused (LPBF) Inconel 718. Results showed a high consistency across builds and certain orientations exhibited superior properties.

1. Introduction

Additive Manufacturing (AM) is a technique that enables the manufacture of near-net-shape components by fusing layers of powder by partial or full melting of the material. The powder is melted using a variety of heat sources, each with a different method. These sources typically include an electron beam, laser beam, plasma or electric welding arc. A component that is produced using this method starts off as a 3D CAD model and is built up in the machine chamber where each layer of powder is a 2D slice from the original 3D model (1).

The AM process has attracted an increased interest from the aerospace industry due to the ability to make intricate parts not feasibly possible through traditional means, in a near-net shape manner with minimal post processing or material wastage, thus improving the buy-to-fly ratio. However, given the relative infancy of AM processes, many structures can still contain structural discontinuities such as porosity and lack of fusion features, whilst care needs to be taken when designing the component to ensure the underlying, typically heavily textured and anisotropic, microstructure of the material is best distributed to restrict in-service damage conditions.

Given the potential of AM processes, there is now major demand from industry to understand and characterise the local mechanical properties of discrete locations in intricate build geometries given the evolving microstructures of AM components. The small punch (SP) test is a small scale test technique initially used to evaluate damage to neutron irradiated materials in the nuclear power generation industry and has been used for remnant life evaluation of steels for power generation applications (2). The small volume of material required to manufacture a SP disc specimen means that material can be extracted from real components with small intricate geometries, and therefore, the mechanical property data obtained is clearly more representative of the component being characterised. As such, SP testing presents an attractive testing solution (2).

The AM process chosen for this study is laser powder bed fusion (LPBF). Like most other AM processes, LPBF builds a 3D component layer-by-layer from a CAD file. The powder is then spread evenly onto a retractable build plate using a powder wiper, at which point a laser beam is guided using scanner mirrors and a focusing objective, melting the powder and fusing it together at a temperature exceeding the melting point to achieve complete melting (3). Once each layer has fused, the platform lowers, to allow the next layer of powder to be deposited on top of the previous layer, upon which the process is repeated until the part is completed. During the entire process, the build chamber is filled with an inert gas to lower the oxygen content, reducing the risk of contamination (1).

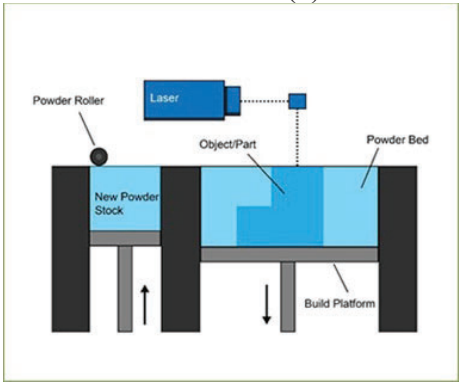

Figure 1. *The Laser Powder Bed Fusion method*

Due to the continuous heat source, a laser in this case, thermal energy is diffused directionally from the rapidly moving laser, towards the build plate. This induces localised melting which is responsible for high cooling rates and therefore a non-uniform solidification of the part. This results in elongated grains formed along the build direction, perpendicular to the build plate, with equiaxed grains more predominant in the plane normal to the build (4). Due to this, the microstructure and mechanical properties of parts built using the LBPF method are strongly build orientation dependent (5). As build consistency is a large concern with additive manufacturing on the build plate, it is also important to observe the consistencies between different builds, to ensure all parts on the build plate, but also parts on separate build plates, have been produced to the same standard.

The purpose of this study is to evaluate the effects of both build orientation and different build runs on IN718 samples produced using the LPBF technique. Microstructural and porosity analysis were performed on all specimens, investigating the influence they have on the mechanical performance of the material, as derived by the SP tensile test.

2. Experimental procedure

2.1.Material

The material investigated in this study is the nickel based superalloy Inconel 718 (IN718). This alloy exhibits impressive high temperature strength and excellent corrosion resistance, making it an ideal material for the aerospace industry. The strength of IN718 is due to the formation of gamma double prime (γ'') precipitates, which are coherent with the primary gamma (γ) FCC matrix, causing distortion in the lattice. This induces a coherency strain within the structure, which acts as a further barrier to dislocation movement, therefore increasing the alloy's strength (6). Prior to testing, all specimens were subjected to a standard AMS 5664 heat treatment, with an initial solution heat treatment at 1066°C for 1 hour followed by argon quenching. After this, there was a 2 step ageing heat treatment, which included heating the specimens for 10 hours at 760±10°C, then heating the specimens to 649±8°C for 8 hours, where the ramp between step 1 and step 2 was 1 hour 50 minutes.

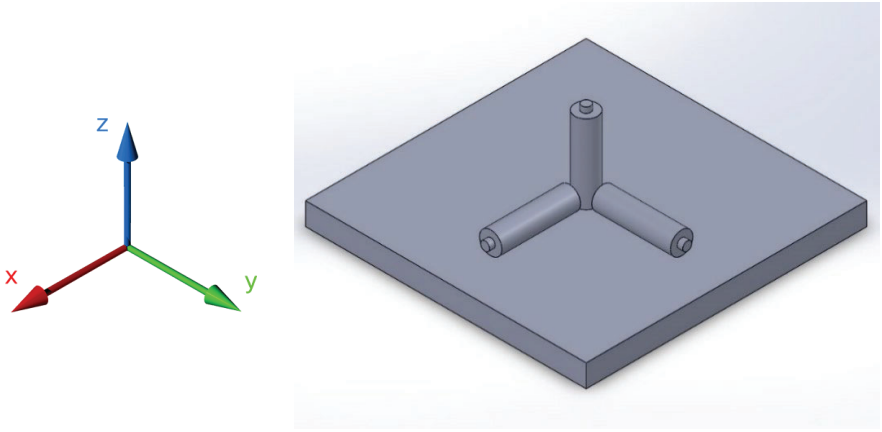

Figure 2. *Build plate design*

IN718 SP test specimens were generated from 2 identical builds, build A and build B, using the same CAD file. One batch of specimens were manufactured on a previous model of the EOS 290 system (Build A) and the other on a newer model of the same machine (Build B). The overall build plate is illustrated in Figure 2, where the build plate comprises of a series of cylindrical rods lying either perpendicular (vertical, z direction) or parallel (horizontal, x and y directions) to the build platform, measuring 70mm long. A small ϕ 8mm, 10mm long coupon is built on the end of each rod, from which SP disc specimens can be extracted from. This research looked at a sample from each of the orientations (x, y, z), where Table 1 represents the specimens and their respective IDs.

Table 1. *Specimen identifications*

Specimen ID	***Build***	***Build orientation***
ZA		*Z*
YA	*A*	*Y*
XA		*X*
ZB		*Z*
YB	*B*	*Y*
XB		*X*

Electron backscattered detection (EBSD) analysis was performed on the surface of all the pre-tested specimens to conduct grain analysis, using the elliptical fit method (7). This allowed for a more accurate representation of grain size and aspect ratio due to the expected elongated grains and anisotropy present in the majority of the specimens. Figure 3 represents the Inverse Pole Figure (IPF) maps generated from this procedure. From the EBSD, values of average local misorientation (KAM – Kernel Average Misorientation) and the sum of all the twin boundaries (Σ3) could also be obtained. Alongside microstructural analysis, porosity calculations were recorded, using a Zeiss Smartzoom 5 optical microscope and ImageJ software, to map the surfaces of the same pre-tested specimens. Results of grain and porosity analysis can be seen in Table 2 below.

Table 2. *Grain and porosity analysis values for IN718 pre-tested SP specimens*

Specimen	***Average grain size (µm²)***	***Aspect ratio***	***Average KAM (°)***	***Σ3 (%)***	***Average pore size (µm²)***	***Porosity Area (%)***
ZA	*159.56*	*0.51*	*0.25*	*0.95*	*40.28*	*0.02*
YA	*302.83*	*0.30*	*0.35*	*0.45*	*51.43*	*0.02*
XA	*434.20*	*0.30*	*0.35*	*0.68*	*35.78*	*0.03*
ZB	*163.34*	*0.50*	*0.25*	*0.83*	*18.28*	*0.03*
YB	*492.38*	*0.14*	*0.25*	*0.32*	*51.21*	*0.02*
XB	*292.09*	*0.32*	*0.35*	*0.65*	*20.93*	*0.02*

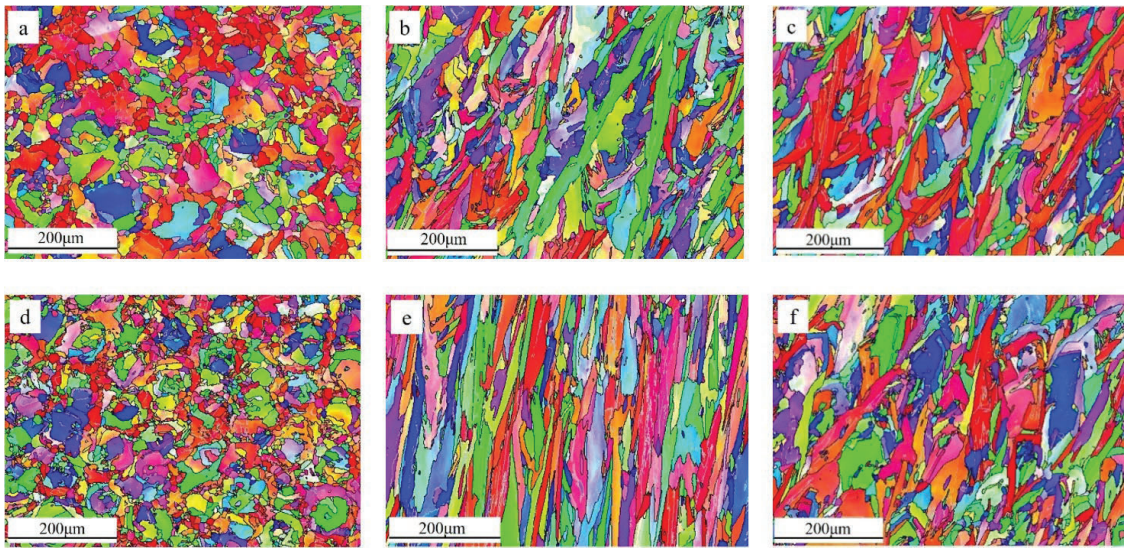

Figure 3. *IPF maps representing the X-Y plane of a) ZA (Z), b) YA (Y), c) XA (X), d) ZB (Z), e) YB (Y), f) XB (X)*

2.2.Small Punch (SP) – Tensile

SP test specimens were extracted by sectioning slices from the ϕ 8mm diameter coupons of material located at the ends of each of the cylindrical rods. SP discs were then prepared by grinding and progressive polishing of the samples to acquire the correct thickness and surface finish of the disc (0.5mm ±0.005mm). This procedure follows the directives outlined in the European Code of Practise for Small Punch Testing (EUCoP) (8) and the soon

to be published EN Standard for Small Punch Testing of Metallic Materials, which require the specimen surface to be finished with 1200 grit paper.

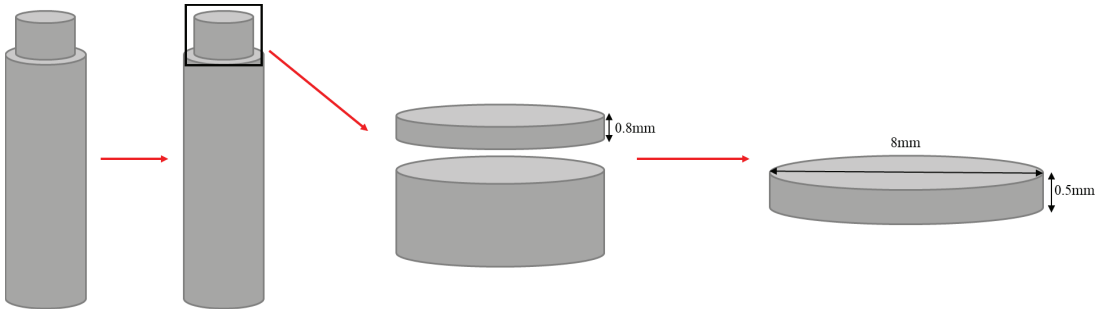

Figure 4. *Small punch specimen preparation*

Once prepared, the SP samples are placed between an upper and lower die, clamping the sample securely. A hemispherical punch, with a diameter of 2.5mm is passed through the die, making contact with the top surface of the sample. A LVDT transducer is placed in contact with the bottom surface of the sample, which records the displacement of the sample during deformation. The punch is then forced onto the sample, imparting a load at a constant displacement rate of 0.5mm/min until there is a 20% drop in the maximum force achieved, at which point the test is terminated. Once the test is completed, a force (F) against displacement *(d)* graph is plotted, akin to a uniaxial tensile test. Figure 5 illustrates the test arrangement for a SP test.

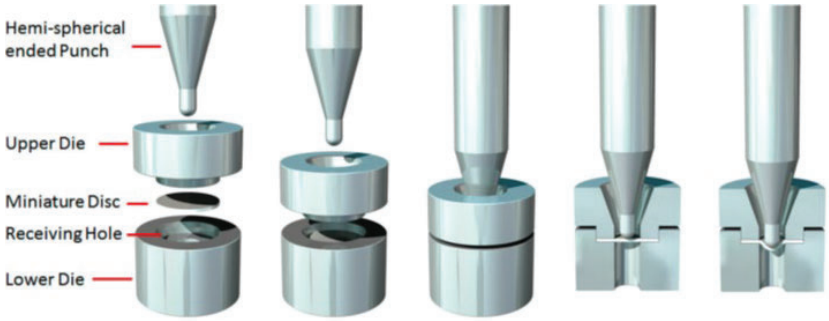

Figure 5. *The small punch tensile test setup (2)*

3. Results and Discussion

3.1 SP tensile (SPT)

Figure 6 graphically represents the mechanical response of the IN718 SP specimens during the SP tensile test, with Table 3 containing the numerical values generated from the tests. The table includes values of F_e (the inflection point between zone 1 – elastic bending, and zone 2 – plastic bending) which is related to the yield strength (9), F_{max} (the maximum force that the punch puts on the surface of the specimen) and d at $0.8F_{max}$ (the displacement of the transducer at the 20% force drop off). When comparing the results for build A, specimen XA, built in the X orientation, has the highest value of F_e (801.1N) and F_{max} (1672.89N), over 100N higher than both ZA and YA. In a similar manner to uniaxial tensile behaviour, these values are at the detriment of d, as the specimen offers the smallest displacement value upon failure, reflecting the most response of the three alternative orientations. The specimens from

build B show a slightly different trend, in that YB has the highest F_{max} (1621.19N), but with the lowest values for F_e and d.

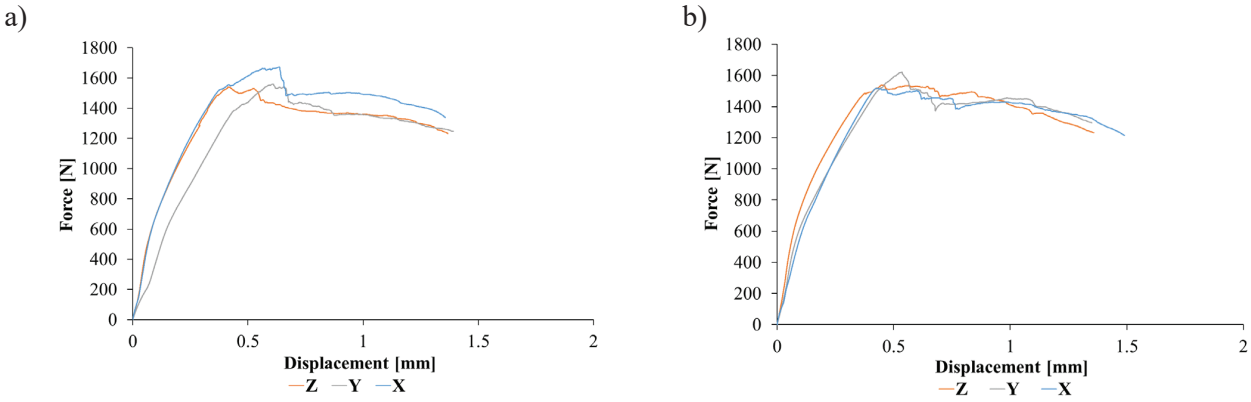

Figure 6. *SP tensile curves a) build A, b) build B*

Table 3*. SP tensile results*

Specimen	***F_e (N)***	***F_{max} (N)***	***d at 0.8F_{max} (mm)***
ZA	*759.00*	*1540.04*	*1.37*
YA	*753.20*	*1558.57*	*1.39*
XA	*801.10*	*1672.89*	*1.36*
ZB	*781.90*	*1539.20*	*1.36*
YB	*643.30*	*1621.19*	*1.35*
XB	*745.50*	*1517.93*	*1.50*

Post-test fractographic analysis was undertaken to study the fracture behaviour of the different specimens (Figure 7). The fracture surfaces across all orientations and build types exhibited a large circular crack due to the plastic flow of the material enveloping the end of the punch, surrounded by a network of smaller cracks that are distributed evenly around the initial crack. This is known as a mixed mode star/cap like failure, which accounts for the initial ductility in the material upon which there is a period of membrane stretching, with secondary cracking then occurring around the periphery of the punch head which is usually more related to brittle type damage, as depicted in Figure 7 d), where the cracks run deeper and thicker than any other sample. Both z specimens have almost identical values of F_{max} and d, with very similar points of inflection. The inflection point of YA is also very similar to both ZA and XA, although the shape of the curve from the start of the test up to F_{max} is very different. There is a steady increase of F with d, although at a lower gradient than ZA and XA, whereas YB has a similar gradient to ZB and XB but with a much lower value for F_e.

Specimens XA and XB however show differences in their behaviors. Even though the fracture surfaces are alike, the curves and material properties are different. YA has an F_e value more than 100N higher than YB, but an F_{max} value approximately 60N lower. Once F_{max} is reached, the response from YA compared to YB is largely different, where YB is similar to those from the x specimens, having a steady decrease in F with increasing d. However, once F_{max} is reached in YA, there is a sudden large decrease in force, followed by a steady decrease.

During the SP tensile test, F is applied as a bi-axial load, compared to a standard tensile test where F is a uniaxial load (10). Therefore, for this study, the microstructures of the X and

Y specimens show elongated grains, perpendicular to the build direction, whereas in the Z built specimens, the microstructure is more equiaxed, as shown in Figure 3 and supported by the aspect ratio values from Table 2. As such, when a SP test is applied to a specimen built in the Z build direction, the material exposed to the load is orthogonal to this orientation and sits on the X-Y plane. This also applies when the X and Y build orientations are SP tested, where the microstructures subjected to loading are aligned in the Y-Z and X-Z planes respectively.

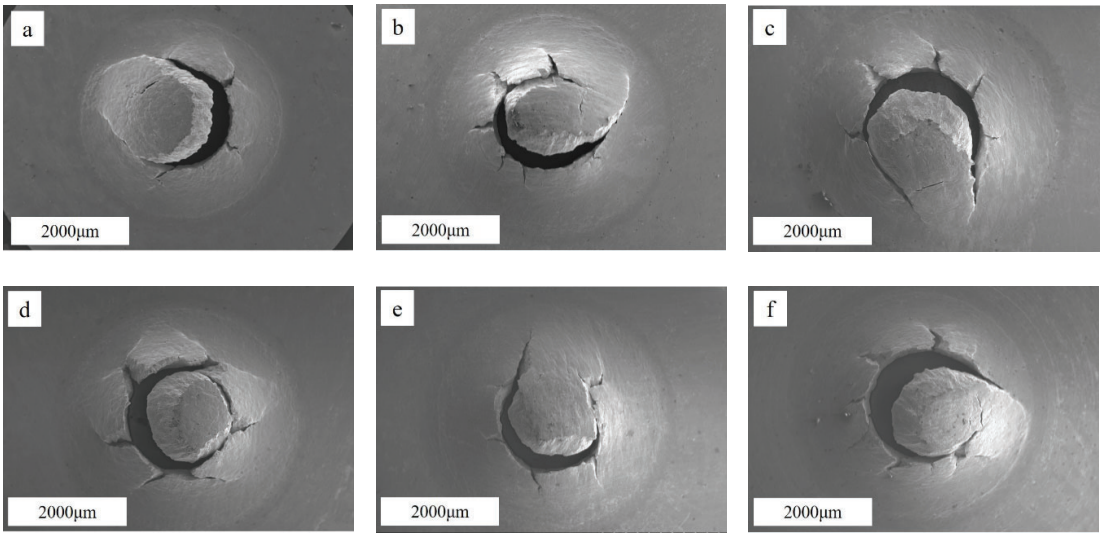

Figure 7. *SP tensile fractography; a) ZA, b), YA, c) XA, d) ZB, e) YB, f) XB*

Given this understanding of the microstructures, and the little deviation seen in the levels of porosity, (Table 2), grain morphology is another possible factor to consider when assessing the SP behaviour of the different materials. As derived from Hall-Petch theory (10), a finer grain structure tends to inhibit dislocation movement as dislocations are blocked by grain boundaries. Therefore, specimens built in the X and Y orientation (YA, XA, YB and XB) should exhibit higher strengths compared to those built in the Z orientation (ZA and ZB) since the microstructure subjected to loading in the Z orientation build is indeed the X-Y plane, the two orientations which offer the largest grain size. For build A, this trend can be seen where ZA has the lowest F_{max} and XA having the largest. However, build B shows slightly different results, where YA has a higher strength than ZB as expected, although XB has the lowest F_{max} of that build. Furthermore, when considering the magnitude of cracking in Figure 7, XB has more secondary cracks than ZB and YB. In general, there is little difference between builds, where all orientations show similar strengths and elongations across both builds. The reason for these slight differences could be attributed to scatter and the sensitivity of the test procedure. Since the SP tensile test characterises such small scale specimens, even the smallest defects or microcracks could have a more considerable influence on mechanical performance than perhaps would be seen in more traditional uniaxial test approaches.

4. Conclusions

In this study, an in depth analysis was performed on LPBF IN718 across two builds to determine the relationship between build orientation, consistency of build run, and mechanical properties. Microscopic methods including SEM, EBSD and optical microscopy analysis were conducted alongside SP tensile testing to draw the following conclusions:

- SP tensile tests were performed successfully to generate values of F_e, F_{max} and d at the 20% drop off from F_{max}.
- Specimens built in the Z orientation produce an equiaxed microstructure, whereas X and Y orientated samples contain elongated grains running parallel to the build direction. Porosity in all 3 orientations was similar but also minimal, making little to no difference on the mechanical response of the IN718 specimens.
- Due to the bi-axial loading in a SP tensile test, two orientations must be considered, where testing in one orientation, for example Z, is testing the response of the other two orientations, in this case, X and Y.
- The X and Y build directions offered a superior SP tensile performance compared to the Z orientated builds, since these orientations tested the smallest combination of grain morphologies (Y-Z plane for X and X-Z for Y) although specimens built in the Z orientation have more consistent results.
- There is a high level of consistency between builds, with the differences in mechanical properties arising from scatter and sensitivity of the SP test.

5. References

1. Antonysamy AA. Microstructure, Texture and Mechanical Property Evolution during Additive Manufacturing of Ti6Al4V Alloy for Aerospace Applications. 2012.
2. Lancaster RJ, Illsley HW, Davies GR, Jeffs SP, Baxter GJ. Modelling the small punch tensile behaviour of an aerospace alloy. Mater Sci Technol (United Kingdom). 2017;33(9):1065–73.
3. Tsai CY, Cheng CW, Lee AC, Tsai MC. Synchronized multi-spot scanning strategies for the laser powder bed fusion process. Addit Manuf. 2019;27(October 2018):1–7.
4. Zhou L, Mehta A, McWilliams B, Cho K, Sohn Y. Microstructure, precipitates and mechanical properties of powder bed fused inconel 718 before and after heat treatment. J Mater Sci Technol. 2019;35(6):1153–64.
5. Poulin JR, Brailovski V, Terriault P. Long fatigue crack propagation behavior of Inconel 625 processed by laser powder bed fusion: Influence of build orientation and post-processing conditions. Int J Fatigue. 2018;116(July):634–47.
6. Kistler NA. Characterization of Inconel 718 Fabricated through Powder Bed Fusion Additive Manufacturing. 2015;1–51.
7. Davies SJ, Jeffs SP, Coleman MP, Lancaster RJ. Effects of heat treatment on microstructure and creep properties of a laser powder bed fused nickel superalloy. Mater Des. 2018;159:39–46.
8. Bruchhausen M, Austin T, Holmström S, Altstadt E, Dymacek P, Jeffs S, et al. European Standard on Small Punch Testing of Metallic Materials. Vol 1A Codes Stand. 2017;(September): V01AT01A065.
9. García TE, Rodríguez C, Belzunce FJ, Suárez C. Estimation of the mechanical properties of metallic materials by means of the small punch test. J Alloys Compd. 2014;582:708–17.
10. Hurst RC, Lancaster RJ, Jeffs SP, Bache MR. The contribution of small punch testing towards the development of materials for aero-engine applications. Theor Appl Fract Mech. 2016;86:69–77.